ACS APPLIED MATERIALS & INTERFACES

Research Article

www.acsami.org

Mixed-Matrix Membranes with Metal–Organic Framework-Decorated CNT Fillers for Efficient CO_2 Separation

Rijia Lin,[†] Lei Ge,*[,†] Shaomin Liu,[‡] Victor Rudolph,[†] and Zhonghua Zhu*[,†]

[†]School of Chemical Engineering, The University of Queensland, Brisbane, Queensland 4072, Australia

[‡]School of Chemical Engineering, Curtin University of Technology, Perth, Western Australia 6102, Australia

Supporting Information

ABSTRACT: Carbon nanotube (CNT) mixed-matrix membranes (MMMs) show great potential to achieve superior gas permeance because of the unique structure of CNTs. However, the challenges of CNT dispersion in polymer matrix and elimination of interfacial defects are still hindering MMMs to be prepared for high gas selectivity. A novel CNT/metal–organic framework (MOF) composite derived from the growth of NH_2-MIL-101(Al) on the surface of CNTs have been synthesized and applied to fabricate polyimide-based MMMs. Extra amino groups and active sites were introduced to external surface of CNTs after MOF decoration. The good adhesion between the synthesized CNT-MIL fillers and polymer phase was observed, even at a high filler loadings up to 15%. Consequently, MMMs containing the synthesized MOF/CNT composite exhibit not only a large CO_2 permeability but also a high CO_2/CH_4 selectivity; the combined performance of permeability and selectivity is even above the Robeson upper bound. The strategy of growing MOFs on CNTs can be further utilized to develop a more effective approach to further improve MMM performance through the decoration of MOFs on existing fillers that have high selectivity to specific gas.

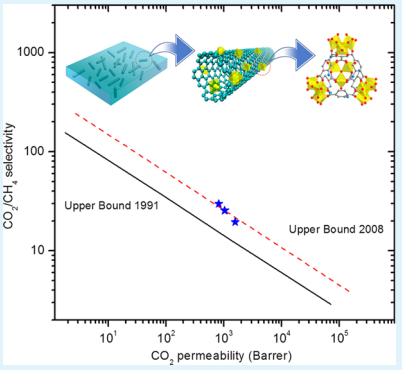

KEYWORDS: *mixed-matrix membranes, carbon nanotubes, metal–organic frameworks, surface decoration, high-performance separation*

1. INTRODUCTION

Gas separation utilizing polymeric membranes has emerged as an efficient process with significant technical and commercial impact.[1,2] Nonetheless, most of the current polymeric membranes are limited by a trade-off between permeability and selectivity, referred as Robeson upper bound: the more permeable polymeric membranes are, the less selective and vice versa.[3,4] In recent years, a breakthrough has been made by embedding filler materials such as inorganic particles into the polymeric matrix. The resultant mixed-matrix membranes (MMMs) combine the advantages of both inorganic particles and polymer membranes, providing the high separation capabilities of the filler particles with good processability and mechanical properties of the polymer.[5,6]

Among the fillers, carbon nanotubes (CNTs) have been widely applied because of their unique structure.[7,8] In particular, gas transport through the CNT tunnels is dramatically accelerated because of the smooth internal walls, conferring on CNT-modified membranes the potential for superior gas permeance.[9,10] However, as with many other nanomaterials, the CNTs are hydrophobic and preferentially aggregate and entangle together. This difficulty in dispersion remains an obstacle impeding their use for highly selective MMM gas separation.

To improve the CNT dispersion quality in the polymer matrix and eliminate interfacial defects, various surface modification strategies have been explored.[11,12] One feasible approach is to graft functional groups on the CNTs exterior surface, which is frequently performed by strong acid treatment.[13,14] Surface functionalization or doping is an effective strategy not only to improve the dispersion quality but also to increase the penetrates' solubility in the composite membranes; in particular, functional groups carrying partial charges can act as the anchor sites to absorb strongly polar gases such as CO_2.[7,15] However, these methods sometimes damage the integrity of the CNTs making them inappropriate for use as the filler for MMM preparation.

Apart from grafting organic functional groups or metal doping, an alternative is to decorate metal–organic frameworks (MOFs) on CNTs, which acts to improve the adsorption selectivity of CNTs.[16] In the previous studies, MOF based composites such as MOF-zeolite and MOF-silica have also been used to fabricate MMMs.[17−19] The incorporation of MOF made zeolite or silica more compatible with polymer. The MMMs exhibited good interaction between polymers and these composite fillers. As a novel group of porous hybrid materials, MOFs can be grown from the precursors of metal and organic linkers, which possess well-defined pore structure, high surface area, and high adsorption affinity/selectivity.[20] Additionally, desired functionalities of MOFs can be easily achieved during

Received: March 27, 2015
Accepted: June 19, 2015
Published: June 19, 2015

DOI: 10.1021/acsami.5b02680
ACS Appl. Mater. Interfaces 2015, 7, 14750−14757

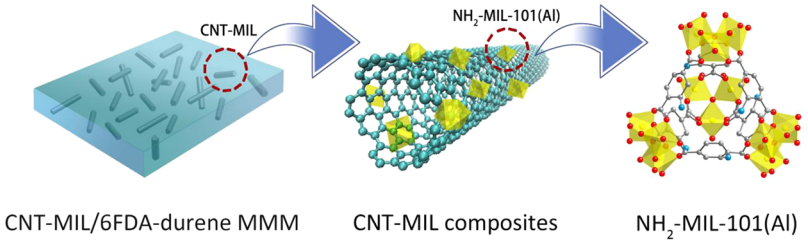

Figure 1. Schematic diagram of 6FDA-durene MMM containing NH_2-MIL-101(Al)-decorated CNTs (Al, yellow; C, gray; O, red; and N, blue).

the synthesis process with different organic linkers, such as $-NH_2$, and $-COO$. By controlling the atomic ratios of metal−organic linkers, a variety of structures with different adsorpability and selectivity for specific gases can be flexibly synthesized.

In this work, we report the use of a novel MMM filler derived from in situ growth of MOFs on the external surface of the CNTs to improve separation performance. NH_2-MIL-101(Al), an MOF based on the MIL-101 topology that presents high sorption selectivity of CO_2, was chosen.[21] CNTs well-covered with MOFs were successfully prepared. NH_2-MIL-101(Al) introduced amino groups and active sites to the external surface of CNTs. The MMMs were fabricated by dispersing the synthesized MOF/CNT composite into 6FDA-durene polyimide (Figure 1).

2. EXPERIMENTAL SECTION

2.1. Materials. Aluminum chloride hexahydrate ($AlCl_3{\cdot}6H_2O$), 2-amino terephthalic acid (NH_2-H_2BDC), 4, 4′-(hexafluoroisopropylidene) diphthalic anhydride (6FDA), 2,3,5,6-tetramethyl-1,3-phenyldiamine (durene), triethylamine, acetic anhydride, N,N-dimethylformamide (DMF), N,N-dimethylacetamide (DMAc), and acetone were supplied by Sigma-Aldrich. The multiwalled CNTs (MWCNTs) produced from methane decomposition over a Fe catalyst in a fluidized-bed reactor were supplied by Tsinghua University, China. The purity in pristine samples exceeded 95 wt %. The orientation of the carbon layers in a typical CNT is parallel to its axis. The external diameter of CNTs is around 30 nm.

2.2. Synthesis of NH_2-MIL-101(Al). NH_2-MIL-101 was synthesized on the basis of a technique reported elsewhere.[21] A 0.119 g amount of $AlCl_3{\cdot}6H_2O$ and 0.131 g of H_2BDC were dissolved into 70 mL of DMF. After 30 min of stirring, the mixture was transferred into a Teflon-lined stainless-steel autoclave and heated at 130 °C for 6 h. After the hydrothermal reaction, NH_2-MIL-101(Al) was separated by centrifugation and washed in acetone three times, with the product finally dried at 180 °C under vacuum for 18 h.

2.3. Synthesis of Carbon Nanotubes and NH_2-MIL-101(Al) Composites. Before synthesis of NH_2-MIL-101(Al)/CNT composites, the carboxyl-modified CNTs were prepared according to a method reported elsewhere.[22] A quantity of CNTs (0.5 g) was sonicated in a 300 mL mixture of concentrated H_2SO_4 (98 vol %)/HNO_3 (70 vol %, 3:1) for 3 h at 60 °C. Subsequently, the sample was washed with deionized water in several centrifugation/redispersion cycles and filtered, followed by drying under vacuum. This procedure provides CNTs with oxidized carboxylic groups on the outer walls (referred as CNT-COOH).

All NH_2-MIL-101(Al)/CNT composites were also prepared under the same solvothermal procedures of NH_2-MIL-101(Al), except for adding 40 mg of CNT-COOH to DMF by repeated sonication and stirring prior to adding H_2BDC. The synthesized NH_2-MIL-101(Al)/CNT composite was referred as CNT-MIL. The mass ratio of CNT in composite is calculated on the basis of the weight loss from element analysis.

2.4. Synthesis of 6FDA-Durene Polyimide. The preparation of 6FDA-durene polyimide (Figure 2) was carried out by chemical imidization using the same method as reported elsewhere.[23,24] A 1.426

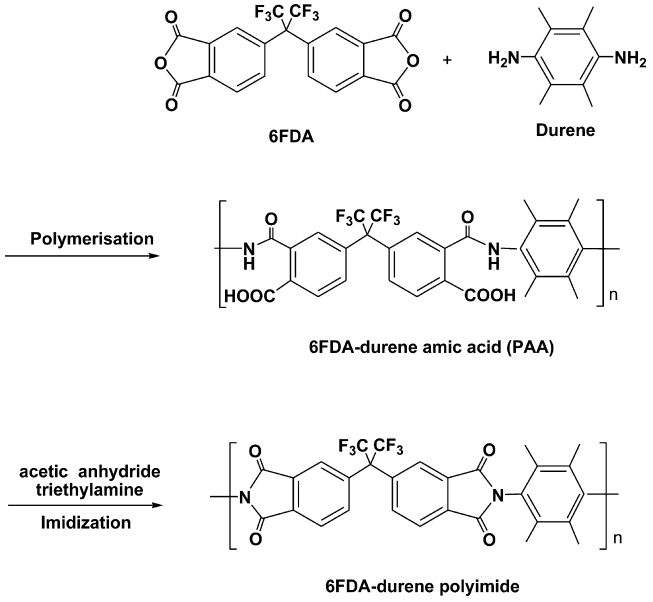

Figure 2. Multistaged 6FDA-durene polyimide synthesis.

g quantity of durene was dissolved into 10 mL of DMAc. Once the durene was fully dissolved, 3.861 g of 6FDA powder was added, followed by addition of 5 mL of DMAc. The mixture was stirred under nitrogen at room temperature for 24 h to form polyamic acid. Next, a mixture of triethylamine (3.2 mL) and acetic anhydride (1.2 mL) was added. The combined mixture was stirred under nitrogen at room temperature for another 24 h. The final polymer was precipitated in methanol, washed several times with methanol, and dried at 180 °C under vacuum for 18 h. The polyimide product is referred as 6FDA-durene.

2.5. Membrane Preparation. For pure 6FDA-durene membrane fabrication, 0.45 g 6FDA-durene membrane was dissolved in 3 mL of DMF at room temperature and stirred until a clear solution was obtained. The resulting solution was cast onto a clean glass substrate, followed by drying at 180 °C for 24 h in a vacuum oven. For the MMMs, a certain amount of as-synthesized CNT-MIL, CNT-COOH, or NH_2-MIL-101(Al) was suspended in DMF under sonication. A 0.45 g quantity of 6FDA-durene was added to this suspension, and the suspension was further stirred for 6 h. The resulting mixture was cast and dried at 180 °C for 24 h under vacuum to form MMM. The loadings of CNT-MIL and CNT-COOH in MMMs were adjusted to 5, 10, and 15 wt % for the purposes of this study, on the basis of eq 1.

$$\phi = \frac{m_{\text{filler}}}{m_{\text{filler}} + m_{\text{6FDA-durene}}} \quad (1)$$

where m_{filler} and $m_{\text{6FDA-durene}}$ are the mass of CNT-MIL/CNT-COOH filler and 6FDA-durene in the MMMs, respectively.

The thickness of pure 6FDA-durene and MMMs were measured using a micrometer within the range of 20−40 μm. Before gas permeation tests and characterization, the membranes were stored with desiccant.

DOI: 10.1021/acsami.5b02680
ACS Appl. Mater. Interfaces 2015, 7, 14750−14757

2.6. Characterization. The X-ray diffraction (XRD) data were obtained from a Bruker Advanced X-ray Diffractometer (40 kV and 30 mA) with Cu Kα (λ = 0.15406 nm) radiation at a scanning rate of 1° min^{-1} from 2 to 40°. The morphologies of the samples were obtained with a JEOL JSM7100 scanning electron microscope (SEM) at 8 kV. High-resolution transmission electron microscopy (HRTEM) was performed on a JEOL JEM-2100 microscope, with accelerating voltages of 200 kV. The samples were dispersed by sonication in ethanol, deposited on a holey-carbon TEM grid, and dried prior to examination.

A Flash EA 1112 CHNS-O analyzer (Thermo Electron) was used to quantify the content of hydrogen, carbon, and nitrogen in CNT-COOH and CNT-MIL composites. The content of NH_2-MIL-101 in the composites can be calculated from the weight percentage of nitrogen by solving eqs 2 and 3

$$NH_2\text{-MIL-101\%} + \text{CNT-COOH\%} = 1 \tag{2}$$

$$\text{CNT-COOH\%} \times N_{\text{CNT-COOH}}\% + NH_2\text{-MIL-101\%} \times \frac{MW_{NH_2\text{-MIL-101}}}{MW_N \times 4} = N_{\text{CNT-MIL}}\% \tag{3}$$

where $N_{\text{CNT-MIL}}$% and $N_{\text{CNT-COOH}}$% are the weight percentages of nitrogen in CNT-MIL and CNT-COOH samples, respectively. $MW_{NH_2\text{-MIL-101}}$ is the molecular weight of NH_2-MIL-101, and MW_N is the atomic weight of nitrogen. $MW_{NH_2\text{-MIL-101}}$ is calculated according to the formula for NH_2-MIL-101 referred to in the literature.[21]

The N_2 adsorption isotherms were measured via a Micromeritics TriStar II 3020 apparatus at 77 K after degassing the sample at 200 °C for 18 h. BET surface area is calculated over the range of relative pressures between 0.05 and 0.15. After N_2 adsorption, the samples were regenerated at 200 °C under a pressure of 10 mTorr until no further pressure drop was observed. Then, the adsorption isotherms of CO_2 and CH_4 at 298 K were measured using the same instrument. The desorption isotherms of CO_2 and CH_4 were obtained by gradually decreasing the system pressure. The adsorption selectivity of CO_2 to CH_4 (S) is calculated according eq 4:

$$S = \frac{q_{CO_2}/q_{CH_4}}{p_{CO_2}/p_{CH_4}} \tag{4}$$

where S is the relative selectivity value, q is the amount of adsorbed gas (cm^3 g^{-1}), and p is the absolute gas pressure (kPa).

The high-pressure sorption of CO_2 and CH_4 was measured in BEL-BG using a magnetic suspension balance (Rubotherm). About 0.7 g of pure 6FDA-durene or MMMs was degassed at 80 °C under vacuum for 2−4 h before adsorption.

2.7. Permeation Test. A variable feed pressure and the constant volume permeation system was used to measure the gas permeation of pure 6FDA-durene and MMMs, as described elsewhere.[25] The membranes were held under vacuum for approximately 5 min to achieve a steady state before the exposure to the selected gas. Before switching to the feed gas, the membrane has to be degassed for some time to ensure the complete desorbtion of initial permeate gas. The test was held at 25 °C under 2 atm feed pressure. Gas permeability values and deviation were calculated from permeation tests from three membranes of each loading.

The permeation coefficient is calculated using the following equation:

$$P = \frac{273.15 \times 10^{10}}{760AT} \frac{VL}{\frac{P_0 \times 76}{14.7}} \frac{dp}{dt} \tag{5}$$

where P is the permeation coefficient in barrer (1 barrer =1 × 10^{-10} cm^3 (STP) cm cm^{-2} s^{-1} cm Hg^{1-}), A is the effective area of the membrane (cm^2), T is the absolute temperature (K), V is the dead volume of the downstream chamber (cm^3), L is the membrane thickness (cm), P_0 is the feed pressure (psi), and dp/dt is the steady rate of pressure increase in the downstream side (mm Hg s^{-1}).

The ideal selectivity for two gases is determined as

$$\alpha = \frac{P_A}{P_B} \tag{6}$$

where P_A and P_B are the permeation coefficients of pure gases A and B, respectively.

For mixed-gas permeation, 50/50% CO_2/CH_4 gas mixture was fed at 3 atm to the retentate side of the membrane, whereas the permeate side of the membrane was swept with Ar at 1 atm. Gas composition in the permeate side was analyzed by a gas chromatograph (Shimadzu GC-8A), and the mixture gas selectivity was calculated accordingly. The separation factor $\alpha_{a,b}$ shows the ability of a membrane to separate binary gas mixture, and it is defined as

$$\alpha_{a,b} = \frac{y_{a,\text{permeate}}/y_{b,\text{permeate}}}{y_{a,\text{retentate}}/y_{b,\text{retentate}}} \tag{7}$$

where $y_{a,\text{permeate}}$ and $y_{b,\text{permeate}}$ are the molar ratios of the components A and B, respectively, in permeate and $y_{a,\text{retentate}}$ and $y_{b,\text{ retentate}}$ are the molar ratio of components A and B, respectively, in retentate.[26]

3. RESULTS AND DISCUSSION

The X-ray diffraction (XRD) patterns of pure NH_2-MIL-101(Al) and CNT-MIL composite samples indicate the existence of the well-defined NH_2-MIL-101(Al) in the as-synthesized CNT-MIL (Figure 3).[27] Compared to pure NH_2-MIL-101(Al), the nucleation sites on the CNT surface produced smaller NH_2-MIL-101(Al) crystals (Figure 4). The "grape bunch" morphology is observed. The NH_2-MIL-101(Al) crystals cover the external surface of the CNTs, as illustrated by scanning electron microscopy (SEM) images in Figure 4b. HRTEM was also applied to reveal the morphology of CNT-MIL (Figure S1). It can be observed that MOF particles are grown on the outer surfaces of CNTs with the particle size at around 50 nm, which is in line with the SEM results (Figure 4). The CNT internal channels are hollow, and there is no evidence for the confined growth of MOFs inside CNTs. Similar morphology has also been observed in our previous studies on MOFs/CNTs composites.[16,28] The content of NH_2-MIL-101(Al) in the CNT-MIL composite is 48.3 wt % as calculated from elemental analysis (Table S1). The BET surface area of pure NH_2-MIL-101(Al) and CNT-MIL measured from

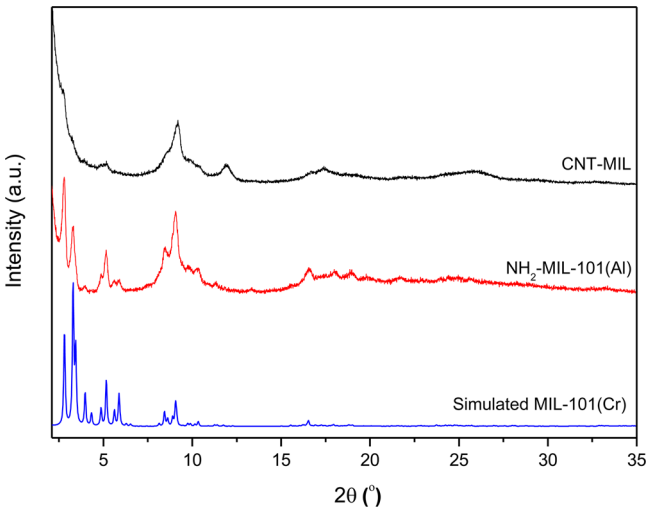

Figure 3. XRD patterns of NH_2-MIL-101 (Al), CNT-MIL composite, and simulated MIL-101(Cr).

DOI: 10.1021/acsami.5b02680
ACS Appl. Mater. Interfaces 2015, 7, 14750−14757

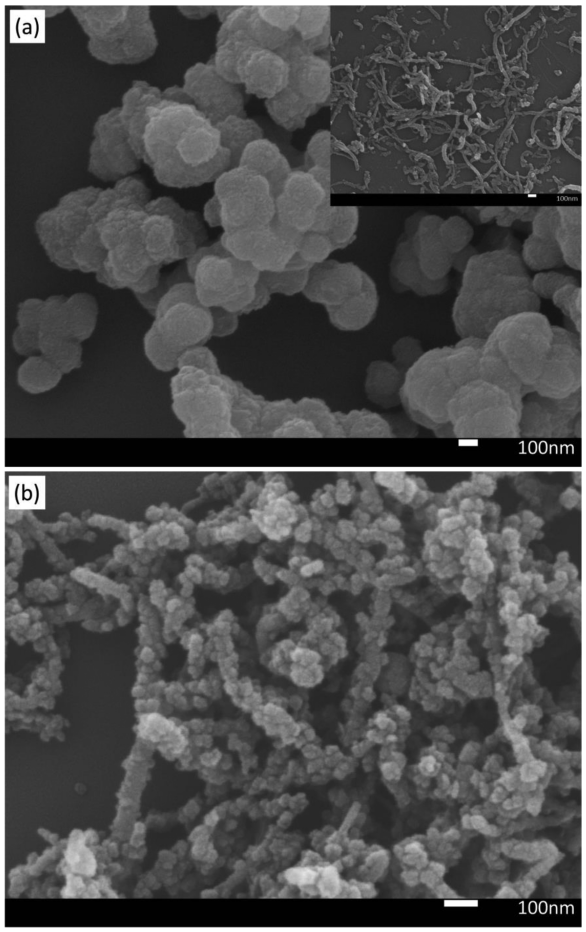

Figure 4. SEM images of (a) NH_2-MIL-101(Al), with CNT-COOH (inset), and (b) CNT-MIL composite.

the N_2 adsorption/desorption isotherms are 1309 and 651 $m^2 g^{-1}$, respectively. CO_2 and CH_4 adsorption isotherms of CNT-COOH, NH_2-MIL-101(Al), and CNT-MIL measured at 298 K are shown in Figure 5. CNT-MIL displays both CO_2 capacity and CO_2/CH_4 ideal selectivity (ratio of the single-component adsorption capacities) that are higher than those of CNT-COOH. At 101 kPa and 298 K, CNT-MIL exhibited an ideal

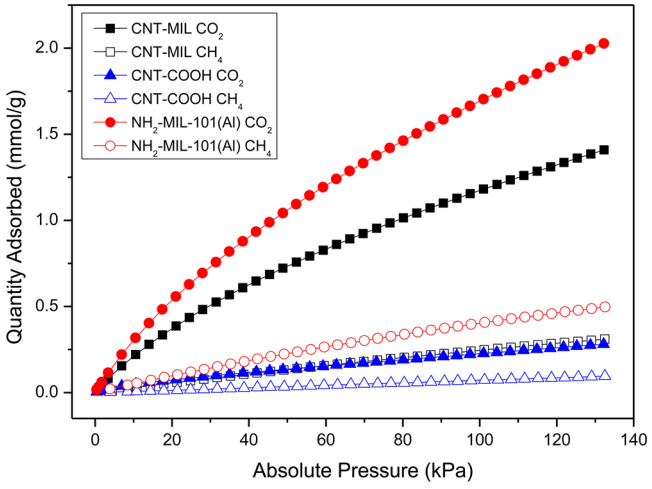

Figure 5. CO_2 and CH_4 adsorption isotherms of CNT-COOH, NH_2-MIL-101(Al), and CNT-MIL at 298 K.

selectivity of 4.75 for CO_2 over CH_4, compared to 3.13 and 4.18 for CNT-COOH and NH_2-MIL-101, respectively. The MOF nanocrystals or functional groups on the external surface of CNTs are expected to induce charge transfer between modification sites and CNTs, thus decreasing the electrostatic potential on the CNT surface, leading to different adsorption selectivity, and contributing to selectivity enhancement by varying solubility.[25]

The SEM images of CNT-MIL/6FDA-durene MMMs cross sections (Figure 6) show good interfacial contact between the CNT-MIL particles and polymer matrix, with no observable interfacial gap. In contrast to the denser cross section of pure 6FDA-durene membrane (Figure 6a), the presence of the concentric cavities in the MMMs indicates that there is strong interfacial interaction between CNT-MIL particles and 6FDA-durene.[29,30] The cross sections of CNT-COOH/6FDA-durene MMMs (Figure S3) have morphology similar to that of CNT-MIL/6FDA-durene MMMs. Compared to CNT-MIL/6FDA-durene MMMs, more severe agglomerations of nanotubes (Figure S4) occurred in CNT-COOH/6FDA-durene MMMs at high loading (>5 wt %). Similar CNT aggregation in MMMs can also be observed in previous literature.[13,15]

Single-gas permeation was used to evaluate the performance of the as-synthesized membranes. Figure 7 shows the gas permeability and selectivity of the pure polymeric membrane. The gas permeance of CO_2 from the pure 6FDA-durene is 618 barrer with CO_2/CH_4 selectivity of 21.6. These results are consistent with the published values of 6FDA-durene membrane.[31] For both CNT-MIL and CNT-COOH MMMs, the permeability of all the gases increased with the filler loading. For instance, a loading at 15 wt % increased the CO_2 permeability of both CNT-MIL and CNT-COOH MMMs by a factor up to 2.5 compared to that of the pure polymeric membrane. Inorganic fillers can disrupt the polymer chain packing, thus creating more free volume, which provides more channels for gas diffusion and achieves higher permeability of the resultant membranes.[32] The permeability enhancement of MMMs can be attributed to the larger free volume introduced by the incorporation of CNTs, the interfacial space between polymer and fillers, and the tunnels provided by the CNTs that can serve as fast channels for gas permeation.

In contrast, the ideal selectivity of the MMMs varies with different fillers and loadings. CNT-COOH/6FDA-durene MMMs exhibit much lower ideal selectivity values than those of the pure polymer because of the lack of sufficient CO_2 selective groups on the surface of CNT-COOH in the polymer matrix. Under such circumstances, nonselective voids are produced on the interface between filler particles and the polymer, resulting in increased extra free volume but cutting down the gas selectivity. Similar observations of reduced selectivity by incorporating functionalized CNT into polymer matrix have also been found previously.[7,15] The reduction of CO_2/CH_4 selectivity was also observed in NH_2-MIL-101(Al) MMMs, which is attributed to the interfacial voids formed between filler and polymer (Table S2 and Figure S5). The "sieve in a cage" morphology of NH_2-MIL-101(Al) MMMs is in line with other reported MMMs containing MOF fillers with larger particle size, serving to reduce the separation performance.[32,33] The confined growth of MOFs on CNT external surfaces reduces crystal size, improving the MOF/polymer interface in the subsequent MMM fabrication.[16,34] By decorating MOFs on CNTs, 6FDA-durene MMMs containing 5 and 10 wt % CNT-MIL provide higher CO_2/CH_4 selectivity

DOI: 10.1021/acsami.5b02680
ACS Appl. Mater. Interfaces 2015, 7, 14750−14757

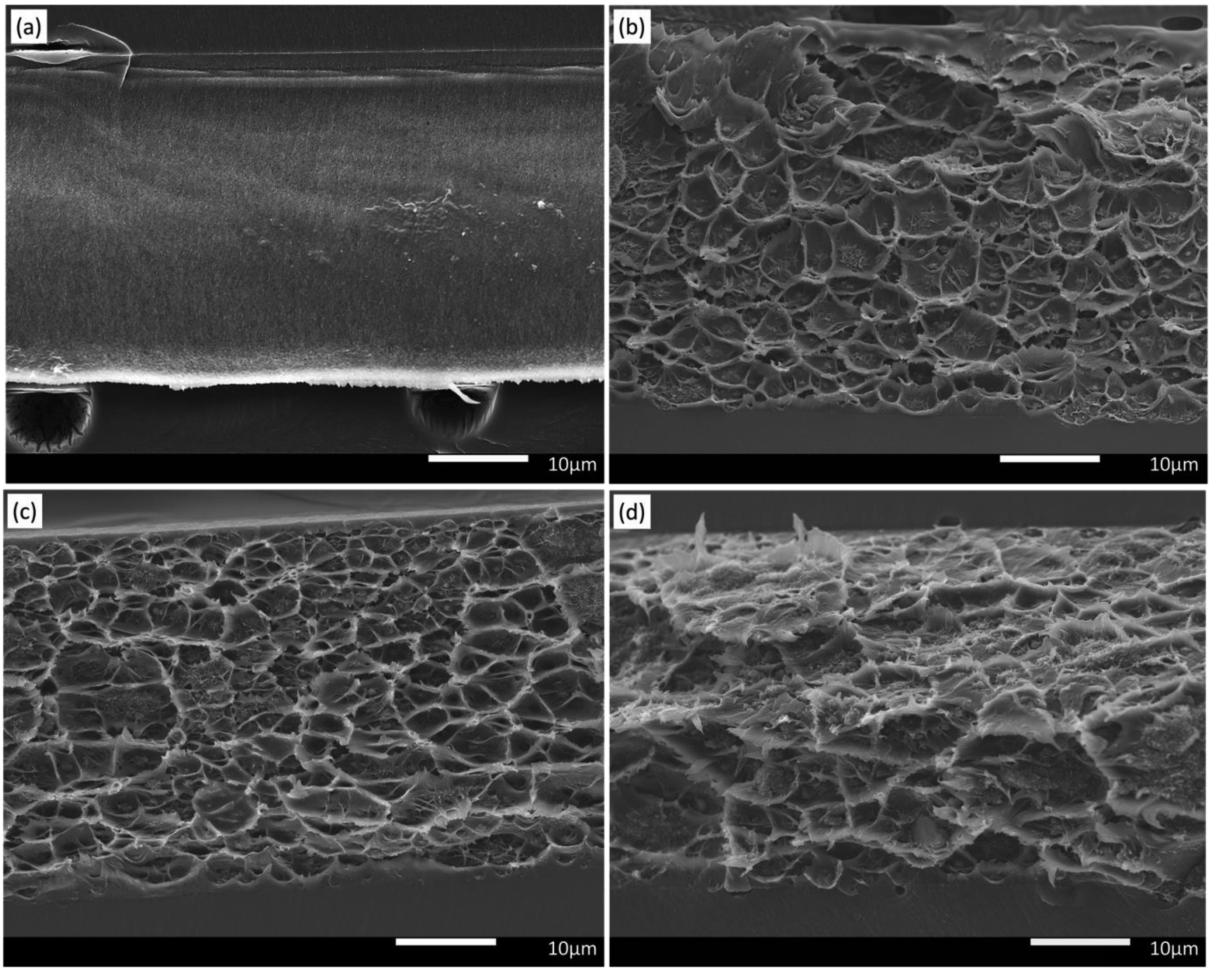

Figure 6. SEM images of (a) pure 6FDA-durene and (b–d) CNT-MIL/6FDA-durene MMMs. Cross-sectional images show samples with different amounts of CNT-MIL (b: 5%; c: 10%; d: 15%).

with increased CO_2 permeability fluxes compared to those of pure 6FDA-durene polyimide membrane. At 10 wt % loading of CNT-MIL, the MMM exhibited a high CO_2 permeability of 1037 barrer with a CO_2/CH_4 selectivity of 25.4. The 50/50% CO_2/CH_4 mixed-gas selectivity of 6FDA-durene and CNT-MIL/6FDA-durene MMMs are shown in the Table S3. The binary gas mixture separation on CNT-MIL/6FDA-durene MMMs showed CO_2/CH_4 selectivity similar to the ideal selectivity.

We believe that the significant improvement in separation performance by the decoration of NH_2-MIL-101(Al) on CNTs can be explained as follows. First, MOF decoration on CNTs enlarges adsorption capacity of CO_2 and CH_4 relative to that of CNT-COOH alone (Figure 5). The $-NH_2$ groups in NH_2-MIL-101(Al) facilitate CO_2 adsorption selectivity. In addition, the interaction between NH_2-MIL-101(Al) and CNT may further enhance the CO_2 adsorption selectivity by electrostatic interactions, as observed previously from MOF/CNT composites.[16,34] Second, the adsorption preference by the fillers is expected to enlarge the membrane solubility difference of CO_2 over CH_4.[32]

The gas solubility difference between the pure 6FDA-durene membrane and CNT-MIL/6FDA-durene MMMs was investigated through measuring pressure-dependent membrane gas sorption isotherms up to 30 bar (Figure 8). On the basis of the solution-diffusion model, the penetrants need to dissolve in the membrane materials before diffusing through the membrane under the pressure gradient.[35] Figure 8 shows the CO_2 and CH_4 adsorption results of 6FDA-durene and 10% CNT-MIL/6FDA-durene MMM. The adsorption amount of CO_2 is much higher than that of CH_4 in both membranes, which indicates that these membranes have higher solubilities of CO_2. The gas sorption isotherms exhibit nonlinear pressure dependence, which is characteristic of the dual-mode sorption consisting of Henry's law sorption in the equilibrium region and Langmuir-type sorption in the nonequilibrium region.[36] The former is related to the dissolution of gases into the dense equilibrium structure of rubbery polymers, whereas the latter corresponds to the sorption on the holes or "microvoids" from the nonequilibrium nature of glassy polymers. The dual-mode sorption model is expressed by[37]

$$C = C_D + C_H = k_D p + \frac{C'_H b_p}{1 + b_p} \quad (8)$$

where C is the total gas concentration in a glassy polymer, C_D is the gas concentration based on Henry's law sorption, C_H is the gas concentration based on Langmuir sorption, k_D is the Henry's law coefficient, and b and C'_H are the hole affinity parameter and the capacity parameter, respectively, in the Langmuir model. k_D represents the penetrant dissolved in the polymer matrix at equilibrium, C'_H shows the amount of the nonequilibrium excess free volume in the glassy state, and b

DOI: 10.1021/acsami.5b02680
ACS Appl. Mater. Interfaces 2015, 7, 14750–14757

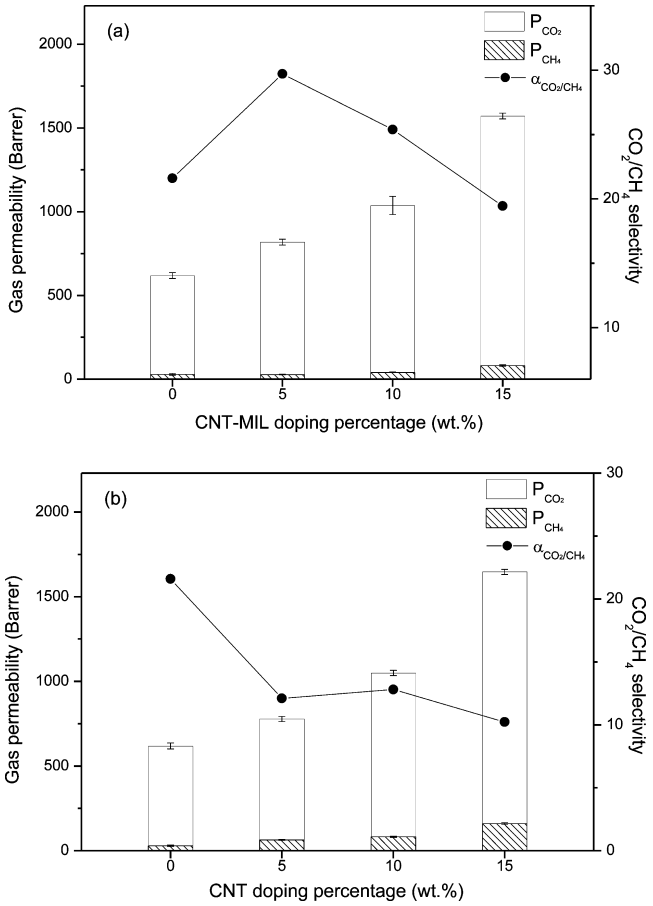

Figure 7. Gas permeability and selectivity of the pure 6FDA-durene membrane, (a) CNT-MIL/6FDA-durene MMMs and (b) CNT/6FDA-durene MMMs.

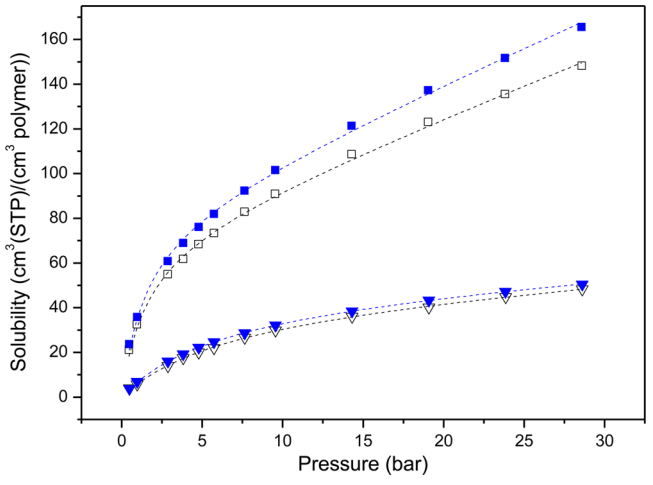

Figure 8. Sorption isotherms of CO_2 (squares) and CH_4 (triangles) in the 6FDA-durene (hollow symbols) and 10% CNT-MIL/6FDA-durene (solid symbols) at 298 K. The dotted lines are fitted lines according to the dual-mode sorption model.

characterizes the sorption affinity for a particular gas−polymer system.[38] The measured CO_2 and CH_4 sorption data can be well fitted by the dual-mode sorption model (Figure 8). The derived parameters are shown in Table 1.

For CO_2 sorption, all parameters of the 10 wt % CNT-MIL/6FDA-durene MMM increase compared to those of the pure

Table 1. Dual-Mode Sorption Parameters for CO_2 and CH_4 in 6FDA-Durene and 10% CNT-MIL/6FDA-durene at 298 K

sample/gases	k_D (cm^3 (STP)/cm^3 bar)	C'_H (cm^3 (STP)/cm^3)	b (bar^{-1})
	6FDA-durene		
CO_2	2.814 ± 0.1224	72.830 ± 3.1327	0.660 ± 0.0808
CH_4	0.480 ± 0.0728	42.547 ± 3.0655	0.149 ± 0.0146
	CNT-MIL/6FDA-durene		
CO_2	3.163 ± 0.1230	81.273 ± 3.1255	0.677 ± 0.0748
CH_4	0.467 ± 0.0212	45.096 ± 0.8585	0.166 ± 0.0045

6FDA-durene membrane (Table 1). The increment of C'_H can be assigned to the disruption of polymer chain packing causing by the CNT-MIL. More free volume is created, resulting in the increase of membrane permeability. The increments of k_D and b reflect the improved CO_2 solubility and sorption affinity of membrane after the introduction of CNT-MIL. In contrast, the k_D for CH_4 decreased. The increment of k_D for CO_2 and the reduction of k_D for CH_4 indicate that more CO_2 and less CH_4 can be dissolved in MMMs with the incorporation of CNT-MIL (Table 1). Similar trends were also observed in other reported MOF MMMs with increased CO_2 solubility selectivity, contributing to membrane separation performance.[39] In the CNT-MIL/6FDA-durene MMMs, the abundant CO_2 selective groups in decorated NH_2-MIL-101(Al) facilitate the augmentation of CO_2 solubility and selectivity in MMMs. To conclude, the improvement of membrane performance by MOF decoration on CNTs can be attributed to the increase of both diffusivity and solubility of CO_2. Compared with the some surface-modification methods (surface functionalization or metal doping),[25] MOF decoration on CNT is a more effective way to improve the membrane performance.

The separation performance of our membranes for the CO_2/CH_4 gas pair is compared with that of other MMMs in the literature with respect to Robeson trade-off line[4] (Figure 9 and Table S4). The performance of CNT-MIL/6FDA-durene

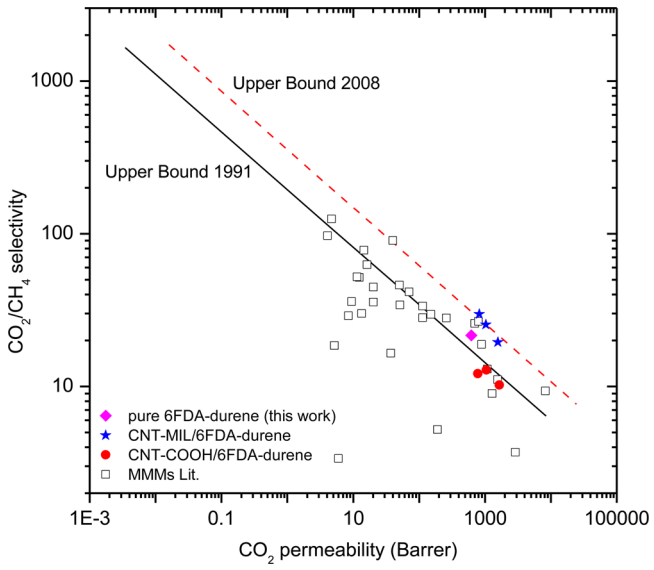

Figure 9. Gas separation performance of the CNT-MIL MMMs for the CO_2/CH_4 gas pair with respect to Robeson trade-off line, compared with the compiled data on other MOF- or CNT-based MMMs in the literature. Detailed citations of MMMs are presented in Figure S6 and Table S4 in the Supporting Information.

DOI: 10.1021/acsami.5b02680
ACS Appl. Mater. Interfaces 2015, 7, 14750−14757

MMMs clearly transcends the 1991 upper bound for polymeric membrane performance. Specifically, CNT-MIL/6FDA-durene with CNT-MIL content of 5 and 10% exhibit excellent CO_2 permeability (818 and 1037 barrer, respectively) and good CO_2/CH_4 selectivity (29.7 and 25.4, respectively), lying on the 2008 upper bound. As shown in Table S4, the as-synthesized CNT-MIL/6FDA-durene MMMs show a higher permeability and better selectivity than the reported MMMs containing MOFs or CNTs alone, indicating potential for CO_2 separation of, for example, biogas or field natural gas. Here the NH_2-MIL-101(Al) decoration and the interaction in CNT-MIL play a critical role for improved CO_2 permeation in the MMMs. The introduction of many and specific functional groups as well as active sorption sites for the target gas has improved the separation performance of the MMMs. The strategy of CNT modification by MOF decoration can be a more effective way to improve the membrane performance of CNT-based MMMs than some organic functionalization methods and to fabricate high-quality MMMs.

4. CONCLUSIONS

Here, we report high-performance MMMs for efficient separation of CO_2/CH_4 by taking advantage of a novel CNT−MOF composite filler. By in situ growth of NH_2-MIL-101(Al) on the external surface of CNTs, amino groups and active sites were introduced. The synthesized CNT-MIL fillers showed good adhesion with the polymer matrix even at a high loading. MMMs containing CNT-MIL displayed significant improvement in both gas permeance and CO_2 selectivity compared to pure 6FDA-durene polyimide membrane. In contrast, 6FDA-durene MMMs with pure CNTs showed lower CO_2 selectivity over CH_4. The extra filler/polymer interface and polar groups provided by MOFs are key factors contributing to efficient CO_2 separation in CNT/polymer MMMs. The strategy we have shown here may lead to the development of a more effective way to further improve MMMs performance through the modification of MOFs on existing fillers that have larger adsorption differences to specific gases. The developed CNT−MOF composites can also be promising for application in adsorption, sensing, and electrochemical reactions.

■ ASSOCIATED CONTENT

Supporting Information

SEM images of CNT-COOH, CNT-COOH/6FDA-durene MMMs and NH_2-MIL-101/6FDA-durene MMM, element analysis of CNT-COOH and CNT-MIL, N_2 adsorption/desorption isotherms of NH_2-MIL-101(Al) and CNT-MIL, gas permeability and selectivity of NH_2-MIL-101/6FDA-durene membrane, and CO_2/CH_4 separation data for other MMMs reported in literature. The Supporting Information is available free of charge on the ACS Publications website at DOI: 10.1021/acsami.5b02680.

■ AUTHOR INFORMATION

Corresponding Authors

*E-mail: l.ge@uq.edu.au.
*Email: z.zhu@uq.edu.au. Tel.: +61 733653528. Fax: +61 733654199.

Notes

The authors declare no competing financial interest.

■ ACKNOWLEDGMENTS

Z.Z. would like to thank the financial support from Australian Research Council Future Fellowship Project FT120100720, and R.L. acknowledges additional financial support from a CSC scholarship from China.

■ REFERENCES

(1) Nasir, R.; Mukhtar, H.; Man, Z.; Mohshim, D. F. Material Advancements in Fabrication of Mixed-Matrix Membranes. *Chem. Eng. Technol.* **2013**, *36*, 717−727.
(2) Scholes, C. A.; Stevens, G. W.; Kentish, S. E. Membrane Gas Separation Applications in Natural Gas Processing. *Fuel* **2012**, *96*, 15−28.
(3) Robeson, L. M. Correlation of Separation Factor versus Permeability for Polymeric Membranes. *J. Membr. Sci.* **1991**, *62*, 165−185.
(4) Robeson, L. M. The Upper Bound Revisited. *J. Membr. Sci.* **2008**, *320*, 390−400.
(5) Dong, G. X.; Li, H. Y.; Chen, V. K. Challenges and Opportunities for Mixed-Matrix Membranes for Gas Separation. *J. Mater. Chem. A* **2013**, *1*, 4610−4630.
(6) Goh, P. S.; Ismail, A. F.; Sanip, S. M.; Ng, B. C.; Aziz, M. Recent Advances of Inorganic Fillers in Mixed Matrix Membrane for Gas Separation. *Sep. Purif. Technol.* **2011**, *81*, 243−264.
(7) Kim, S.; Chen, L.; Johnson, J. K.; Marand, E. Polysulfone and Functionalized Carbon Nanotube Mixed Matrix Membranes for Gas Separation: Theory and Experiment. *J. Membr. Sci.* **2007**, *294*, 147−158.
(8) Ismail, A. F.; Rahim, N. H.; Mustafa, A.; Matsuura, T.; Ng, B. C.; Abdullah, S.; Hashemifard, S. A. Gas Separation Performance of Polyethersulfone/Multi-Walled Carbon Nanotubes Mixed Matrix Membranes. *Sep. Purif. Technol.* **2011**, *80*, 20−31.
(9) Ackerman, D. M.; Skoulidas, A. I.; Sholl, D. S.; Karl Johnson, J. Diffusivities of Ar and Ne in Carbon Nanotubes. *Mol. Simul.* **2003**, *29*, 677−684.
(10) Skoulidas, A. I.; Ackerman, D. M.; Johnson, J. K.; Sholl, D. S. Rapid Transport of Gases in Carbon Nanotubes. *Phys. Rev. Lett.* **2002**, *89*, 185901−185904.
(11) Hirsch, A.; Vostrowsky, O. In *Functional Molecular Nanostructures*; Schlüter, A. D., Ed.; Springer: Berlin Heidelberg, 2005; Vol. *245*, pp 193−237.
(12) Balasubramanian, K.; Burghard, M. Chemically Functionalized Carbon Nanotubes. *Small* **2005**, *1*, 180−192.
(13) Ge, L.; Zhu, Z.; Rudolph, V. Enhanced Gas Permeability by Fabricating Functionalized Multi-Walled Carbon Nanotubes and Polyethersulfone Nanocomposite Membrane. *Sep. Purif. Technol.* **2011**, *78*, 76−82.
(14) Weng, T. H.; Tseng, H. H.; Wey, M.-Y. Preparation and Characterization of Multi-Walled Carbon Nanotube/PBNPI Nanocomposite Membrane for H_2/CH_4 Separation. *Int. J. Hydrogen Energy* **2009**, *34*, 8707−8715.
(15) Kim, S.; Pechar, T. W.; Marand, E. Poly(imide siloxane) and Carbon Nanotube Mixed Matrix Membranes for Gas Separation. *Desalination* **2006**, *192*, 330−339.
(16) Yang, Y.; Ge, L.; Rudolph, V.; Zhu, Z. In Situ Synthesis of Zeolitic Imidazolate Frameworks/Carbon Nanotube Composites with Enhanced CO_2 Adsorption. *Dalton Trans.* **2014**, *43*, 7028−7036.
(17) Zornoza, B.; Seoane, B.; Zamaro, J. M.; Tellez, C.; Coronas, J. Combination of MOFs and Zeolites for Mixed-Matrix Membranes. *ChemPhysChem* **2011**, *12*, 2781−2785.
(18) Sorribas, S.; Zornoza, B.; Téllez, C.; Coronas, J. Mixed Matrix Membranes Comprising Silica-(ZIF-8) Core−Shell Spheres with Ordered Meso−Microporosity for Natural- and Bio-Gas Upgrading. *J. Membr. Sci.* **2014**, *452*, 184−192.
(19) Kudasheva, A.; Sorribas, S.; Zornoza, B.; Téllez, C.; Coronas, J. Pervaporation of Water/Ethanol Mixtures through Polyimide Based Mixed Matrix Membranes Containing ZIF-8, Ordered Mesoporous

DOI: 10.1021/acsami.5b02680
ACS Appl. Mater. Interfaces 2015, 7, 14750−14757

Silica and ZIF-8-Silica Core-Shell Spheres. *J. Chem. Technol. Biotechnol.* **2015**, *90*, 669−677.
(20) Li, J. R.; Sculley, J.; Zhou, H. C. Metal−Organic Frameworks for Separations. *Chem. Rev.* **2012**, *112*, 869−932.
(21) Serra-Crespo, P.; Ramos-Fernandez, E. V.; Gascon, J.; Kapteijn, F. Synthesis and Characterization of an Amino Functionalized MIL-101(Al): Separation and Catalytic Properties. *Chem. Mater.* **2011**, *23*, 2565−2572.
(22) Banerjee, S.; Hemraj-Benny, T.; Wong, S. S. Covalent Surface Chemistry of Single-Walled Carbon Nanotubes. *Adv. Mater.* **2005**, *17*, 17−29.
(23) Liu, Y.; Wang, R.; Chung, T. S. Chemical Cross-Linking Modification of Polyimide Membranes for Gas Separation. *J. Membr. Sci.* **2001**, *189*, 231−239.
(24) Wijenayake, S. N.; Panapitiya, N. P.; Versteeg, S. H.; Nguyen, C. N.; Goel, S.; Balkus, K. J.; Musselman, I. H.; Ferraris, J. P. Surface Cross-Linking of ZIF-8/Polyimide Mixed Matrix Membranes (MMMs) for Gas Separation. *Ind. Eng. Chem. Res.* **2013**, *52*, 6991−7001.
(25) Ge, L.; Zhu, Z.; Li, F.; Liu, S.; Wang, L.; Tang, X.; Rudolph, V. Investigation of Gas Permeability in Carbon Nanotube (CNT)−Polymer Matrix Membranes via Modifying CNTs with Functional Groups/Metals and Controlling Modification Location. *J. Phys. Chem. C* **2011**, *115*, 6661−6670.
(26) Koros, W.; Ma, Y.; Shimidzu, T. Terminology for Membranes and Membrane Processes. *J. Membr. Sci.* **1996**, *120*, 149−159.
(27) Srirambalaji, R.; Hong, S.; Natarajan, R.; Yoon, M.; Hota, R.; Kim, Y.; Ho Ko, Y.; Kim, K. Tandem Catalysis with a Bifunctional Site-Isolated Lewis Acid-Bronsted Base Metal-Organic Framework, NH_2-MIL-101(Al). *Chem. Commun.* **2012**, *48*, 11650−11652.
(28) Ge, L.; Yang, Y.; Wang, L.; Zhou, W.; De Marco, R.; Chen, Z.; Zou, J.; Zhu, Z. High Activity Electrocatalysts from Metal−Organic Framework-Carbon Nanotube Templates for the Oxygen Reduction Reaction. *Carbon* **2015**, *82*, 417−424.
(29) Zhang, Y.; Musselman, I. H.; Ferraris, J. P.; Balkus, K. J., Jr. Gas Permeability Properties of Matrimid® Membranes Containing the Metal-Organic Framework Cu-BPY-HFS. *J. Membr. Sci.* **2008**, *313*, 170−181.
(30) Ordonez, M. J. C.; Balkus, K. J., Jr.; Ferraris, J. P.; Musselman, I. H. Molecular Sieving Realized with ZIF-8/Matrimid Mixed-Matrix Membranes. *J. Membr. Sci.* **2010**, *361*, 28−37.
(31) Lin, W.-H.; Chung, T. S. Gas Permeability, Diffusivity, Solubility, and Aging Characteristics of 6FDA-durene Polyimide Membranes. *J. Membr. Sci.* **2001**, *186*, 183−193.
(32) Ge, L.; Zhou, W.; Rudolph, V.; Zhu, Z. H. Mixed Matrix Membranes Incorporated with Size-Reduced Cu-BTC for Improved Gas Separation. *J. Mater. Chem. A* **2013**, *1*, 6350−6358.
(33) Nik, O. G.; Chen, X. Y.; Kaliaguine, S. Functionalized Metal Organic Framework-Polyimide Mixed Matrix Membranes for CO_2/CH_4 Separation. *J. Membr. Sci.* **2012**, *413−414*, 48−61.
(34) Ge, L.; Wang, L.; Rudolph, V.; Zhu, Z. Hierarchically Structured Metal−Organic Framework/Vertically-Aligned Carbon Nanotubes Hybrids for CO_2 Capture. *RSC Adv.* **2013**, *3*, 25360−25366.
(35) Wijmans, J. G.; Baker, R. W. The Solution-Diffusion Model: a Review. *J. Membr. Sci.* **1995**, *107*, 1−21.
(36) Kanehashi, S.; Nagai, K. Analysis of Dual-Mode Model Parameters for Gas Sorption in Glassy Polymers. *J. Membr. Sci.* **2005**, *253*, 117−138.
(37) Merkel, T. C.; Freeman, B. D.; Spontak, R. J.; He, Z.; Pinnau, I.; Meakin, P.; Hill, A. J. Sorption, Transport, and Structural Evidence for Enhanced Free Volume in Poly(4-methyl-2-pentyne)/Fumed Silica Nanocomposite Membranes. *Chem. Mater.* **2002**, *15*, 109−123.
(38) Paul, D. R. Gas Sorption and Transport in Glassy Polymers. *Bunsen-Ges. Phys. Chem. Ber.* **1979**, *83*, 294−302.
(39) Lin, R.; Ge, L.; Hou, L.; Strounina, E.; Rudolph, V.; Zhu, Z. Mixed Matrix Membranes with Strengthened MOFs/Polymer Interfacial Interaction and Improved Membrane Performance. *ACS Appl. Mater. Interfaces* **2014**, *6*, 5609−5618.

DOI: 10.1021/acsami.5b02680
ACS Appl. Mater. Interfaces 2015, 7, 14750−14757